Available at www.sciencedirect.com

ScienceDirect

journal homepage: www.elsevier.com/locate/he

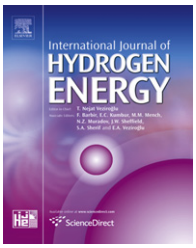

Ultra-sensitive hydrogen gas sensors based on Pd-decorated tin dioxide nanostructures: Room temperature operating sensors

Jun Min Lee [a,1], *Ji-eun Park* [b,1], *Seri Kim* [b], *Sol Kim* [b], *Eunyoung Lee* [a], *Sung-Jin Kim* [b,**], *Wooyoung Lee* [a,*]

[a] *Department of Materials Science and Engineering, Yonsei University, Seoul 120-749, South Korea*
[b] *Department of Chemistry and Nano Science, Ewha Woman's University, Seoul 120-750, South Korea*

ARTICLE INFO

Article history:
Received 25 May 2010
Received in revised form
4 August 2010
Accepted 5 August 2010
Available online 16 September 2010

Keywords:
Tin dioxide
Tin nanoparticles
Pd nanoparticles
Hydrogen gas
Spill-over
Depleted region

ABSTRACT

We have investigated the fabrication of hydrogen gas sensors based on networks of Pd nanoparticles (NPs) deposited tin dioxide nanowires (NWs). SnO_2 NWs with tin NPs attached on the surface were obtained by a simple thermal evaporation of SnO crystalline powders. The tin dioxide NWs were decorated with Pd NPs by the reduction process in Pd ion solution. The sensors showed ultra-high sensitivity ($\sim 1.2 \times 10^5$%) and fast response time ($\sim$2 s) upon exposure to 10,000 ppm H_2 at room temperature. These sensors were also found to enable a significant electrical conductance modulation upon exposure to extremely low concentrations (40 ppm) of H_2 in the air. Our fabrication method of sensors combining with Pd NPs, Sn NPs and n-type semiconducting SnO_2 NWs allows optimized catalytic and depletion effect and results the production of highly-sensitive H_2 sensors that exhibit a broad dynamic detection range, fast response times, and an ultra-low detection limit.

1. Introduction

Hydrogen is one of the most important and promising energy sources for environmentally friendly technologies. One energy application is the hydrogen fuel cell, which efficiently produces electricity and does not require power lines [1–3]. However, hydrogen is flammable and explosive when its concentration exceeds 4% in air [3]. Accurate and fast detection of H_2 is therefore necessary for the extensive adoption of hydrogen use in energy production. Pd is a well-known metal catalyst for H_2 dissociation and also for formation of Pd hydride [4]. Recently, a lattice expansion mechanism for Pd with a fast response time and a high sensitivity has been proposed [5–8]. Penner et al. [5] have fabricated mesoscopic Pd wires for use as H_2 sensors and switches, operated by the lattice expansion of Pd wires. These samples showed a very fast response time but they had a relatively high detection limit of 1% H_2.

Tin dioxide is also widely used as an H_2-sensing material [9–18] because of its simple structure and reaction principles. The reduction/oxidation of the surface of SnO_2 is the main mechanism induced by H_2 at high temperatures [9,13]. Shukla

* *Corresponding author*. Tel.: +82 2 2123 2834; fax: +82 2 312 5375.
** *Corresponding author*. Tel.: +82 2 3277 2335; fax: +82 2 3277 2384.
E-mail addresses: sjkim@ewha.ac.kr (S.-J. Kim), wooyoung@yonsei.ac.kr (W. Lee).
[1] These authors equally contributed to this work.
0360-3199/$ – see front matter © 2010 Professor T. Nejat Veziroglu. Published by Elsevier Ltd. All rights reserved.
doi:10.1016/j.ijhydene.2010.08.026

et al. [11] have modified nano–micro-integrated thin film sensors with indium oxide (In_2O_3)-doped SnO_2. These sensors had a very high sensitivity to H_2 at room temperature, but they exhibited a very slow response time. Pd nanoparticles (NPs) have also been incorporated onto SnO_2 thin films, [12] nanobelts [13], and nanowires (NWs) [14,15] to improve their sensitivities to H_2.

De et al. [10] have synthesized mesoporous PdO-SnO_2 films responding to H_2 at room temperature, and these have shown high sensitivity and selectivity to H_2 down to 500 ppm H_2 at room temperature. However, slow response behaviors have been observed in these sensors. Kolmakov et al. [13] have demonstrated the effect of Pd-doping with individual SnO_2 NWs and nanobelts. Palladium-doping on SnO_2 NWs showed high sensitivity and a fast response compared with those of undoped Pd on SnO_2 NWs, but the operating temperatures of the doped samples were higher than room temperature. In this paper, we report a novel fabrication method of H_2 sensors based on a mixed network of Pd NPs decorated SnO_2 NWs. The SnO_2 network sensors for H_2 detection show ultra-high sensitivity ($\sim 1.2 \times 10^5$%) and a fast response time (~2 s) upon exposure to 10,000 ppm H_2 at room temperature. These sensors also demonstrate a significant electrical conductance modulation upon exposure to extremely low concentrations (down to 40 ppm) of H_2 in air. We discuss the H_2-sensing mechanisms of the SnO_2 network sensors and their performance depending on synthetic conditions.

2. Experimental Procedures

2.1. Synthesis

This approach was based on a thermal vaporization process which is the main mechanism for synthesis and guarantees the achievement of highly pure and catalyst-free nanostructures. Mixtures of SnO_2 NWs and Sn NPs, where Sn NPs are attached on the surface of SnO_2 NWs, were obtained by the simple thermal evaporation of SnO powder in a high-temperature tube furnace equipped with graphitized quartz tube as an inner tube. An alumina boat which contained precursor SnO (3.0 g, 99.99% purity) powder was placed on the inner graphitized quartz tube with diameter of 3 cm. Another alumina boat for product was placed downstream of the flowing Ar gas. No catalyst metal was used for the preparation of the SnO_2 nanostructures. The end of the inner tube was 5 cm from the center of the high-temperature tube furnace, which was heated to 900 °C rapidly under a constant Ar gas flow. Then, the furnace was heated to 1070 °C for an hour and maintained for 3 h at the same gas flow. After the heat treatment, the furnace was cooled to room temperature at a rate of 3 °C/min. After the thermal synthetic reaction, large amounts of SnO_2 NWs with Sn NPs on the surface (hereafter we refer as SnO_2 NWs) were produced on the downstream alumina boat.

Distilled water (30 ml) was added to a three-neck round bottom flask (100 ml) along with a metal precursor material (0.005 mmol) and $PdCl_2$ (palladium chloride, Reagent Plus, 99%). SnO_2 NWs (10 mg, synthesis described above) were then added into the flask. Two drops of HCl (hydrochloric acid, 35%) were also mixed into the Pd reaction flasks in order to balance the pH conditions. These flasks containing the precursor and wires were treated for 30 min in an ultrasonic bath. After sonication, the mixtures of SnO_2 NWs were well dispersed into a metal ion solution. This solution was stirred for an hour under N_2 gas. Subsequently, the solution was reduced by $NaBH_4$ (0.1 mol) at room temperature. Finally, the products were washed with distilled water.

2.2. Device fabrication

In order to fabricate the devices based on the Pd NP-decorated SnO_2 NWs and Sn NPs with decorated Pd NPs, a 20-nm-thick Ti film and a 100-nm-thick Au film were deposited onto a thermally oxidized Si(100) substrate using a direct current magnetron sputtering system with a base pressure of 4×10^{-8} Torr. A combination of photolithography and lift-off techniques was utilized to fabricate the micron-scale Ti/Au electrodes. Then, Pd NP-decorated SnO_2 NWs were dispersed onto the Ti/Au electrodes via micro-pipette drops and ultrasonic spreading of the sample. An effective area of the substrate and sensing materials we used are 7.5 mm × 7.5 mm and 1 mm × 1 mm, respectively.

2.3. H_2 response measurements

The measurement system consisted of a sealed chamber (~250 mL) with a gas inlet and outlet, mass flow controllers for monitoring the ratio of H_2 to air, and digital multimeters connected to a personal computer. Two gases were mixed from different lines and flowed into the chamber through the gas inlet line. Typically maximum flow rates for testing were 1000 sccm Air and 500 sccm 1% H_2 in air. The pressure in the chamber was maintained at near atmospheric pressure. The real-time electrical resistance response to H_2 was measured by the sensors. All data acquisitions were carried out with LabView software through a GPIB interface card. The surface morphology of the samples was observed using field emission scanning electron microscope (FE-SEM, JEOL JSM-600F) at an accelerating voltage of 10 keV and transmission electron microscopy (TEM, JEOL-2010F) using an accelerating voltage of 200 keV.

3. Results and discussion

3.1. Structures and H_2 response properties

Fig. 1 provides a SEM image of SnO_2 NWs mixed with Sn NPs prepared by a simple thermal evaporation method (Fig. 1 a), an HRTEM image of Pd NP-decorated SnO_2 NWs (Fig. 1 b), a schematic image of a SnO_2 network sensor consisting of a mixture of Pd NPs decorated SnO_2 NWs on Au electrodes (Fig. 1 c), and TEM images of a SnO_2 NW with Sn NPs on the surface (Fig. 1 d). The diameters of the SnO_2 NWs and Sn NPs were found to be in the range of tens to hundreds of nanometers. Fourier transforms of the HRTEM images (insets) confirmed that the wires are SnO_2 phase with rutile structure

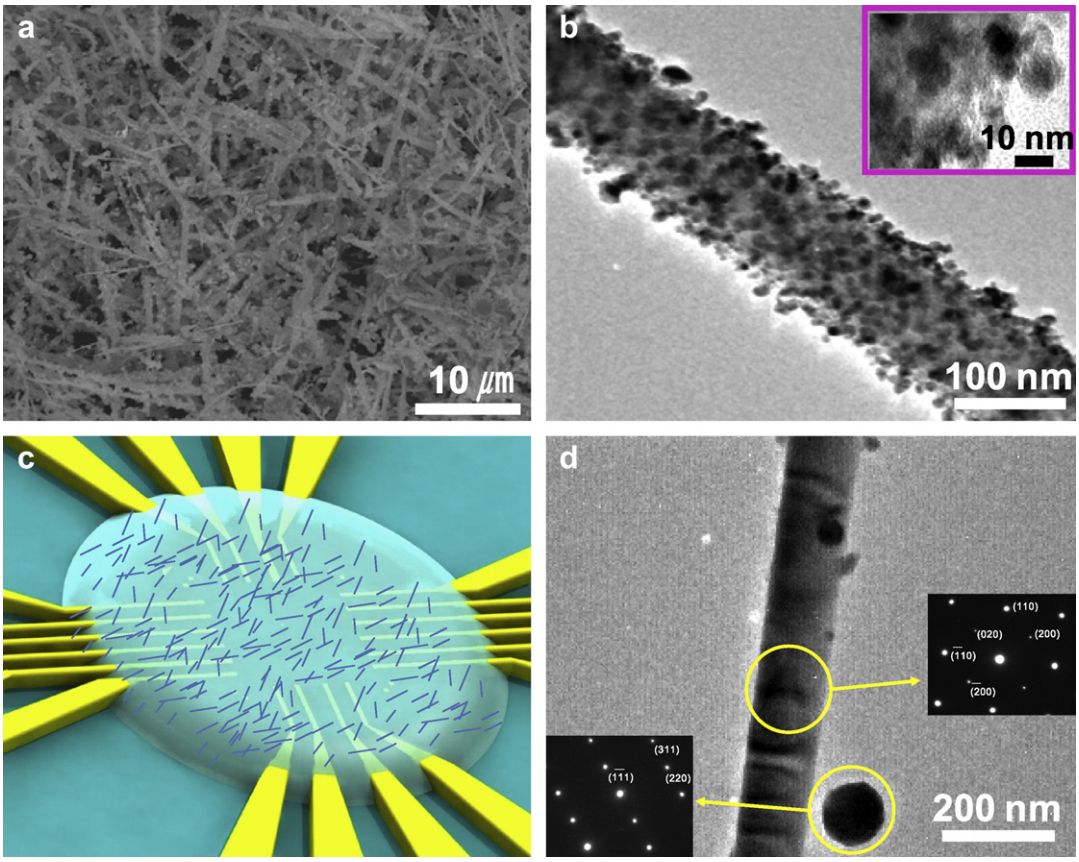

Fig. 1 – (a) A SEM image of SnO_2 NWs and Sn NPs fabricated by a simple thermal evaporation method, (b) a TEM image of a mixture of SnO_2 NWs with functionalized Pd NPs, (c) schematic images of devices prepared by dispersing mixtures of SnO_2 NWs and Sn NPs with functionalized Pd NPs by micro-pipetting on Au electrodes on a substrate, (d) TEM images of a SnO_2 NW with Sn NPs on the surface. The insets of shows selected area electron diffraction (SEAD) patterns indicating tetrahedral rutile SnO_2 with $P4_2/mmm$ symmetry and α-Sn with cubic Fd3m symmetry.

and dots are hexagonal Sn phase. The SnO_2 network sensors were fabricated by dispersing a mixture of the Pd NP-decorated SnO_2 NWs and Sn NPs on Au electrodes.

The SnO_2 network sensors employing mixtures of the Pd NP-decorated SnO_2 NWs and Sn NPs were used to detect H_2 in the concentration range of 40–10,000 ppm at room temperature by measuring changes in their electrical conductance. To measure the variations in their electrical properties with gas absorption and desorption, the SnO_2 network sensors were first exposed to air or nitrogen gas (N_2) to obtain a baseline, then to a designated concentration of H_2, and then back to air or N_2, thus completing one cycle. The transient response properties of the SnO_2 network sensors at various H_2 concentrations are shown in Fig. 2. A representative electrical conductance response of a SnO_2 network sensor to the presence of 10,000 ppm H_2 in air at room temperature is shown in Fig. 2 a, while a real-time conductance response of the SnO_2 network sensor to H_2 in the concentration range of 40–10,000 ppm in air is provided in Fig. 2 b. Variations in H_2 sensitivity as a logarithmic function of H_2 concentration are shown in Fig. 2 c.

The response time can be defined as the time required to reach 36.8% ($= e^{-1}$) of the total change in the electric resistance at a given H_2 concentration [19,20]. As seen in Fig. 2 a, the SnO_2 network sensor exhibited a very fast response time of 2 s. The SnO_2 network sensor showed a large conductance level change, signifying a switch-like property at room temperature, mainly due to heavily decorated Pd NPs on SnO_2 NWs. Moreover, it was also found that the SnO_2 network sensors showed good repeatability in their changes of current without observing major signal variations indicating a poisoning effect. It is well known to occur when high-concentration H_2 is exposed to a sensor under a long-term period [21]. The hydrogen sensing mechanism in the SnO2 network sensor showing "ON–OFF switching" is mainly based on changes in the electrical conductance as the H atoms dissociated from H_2 due to the catalytic activity of Pd NPs and "spill-over" effect with oxygen ions at the surface of SnO_2 [13]. Further details related to the mechanisms of the SnO_2 network sensors will be discussed later. Fig. 2 b illustrates representative electrical conductance in the range of 40–10,000 ppm H_2 for the SnO_2 network sensor in air. The amplitude of the conductance was dependent on the H_2 concentration. As shown in the inset of Fig. 2 b, the SnO_2 network sensor was found to successfully detect H_2 at concentrations down to 40 ppm. The sensitivity variation as

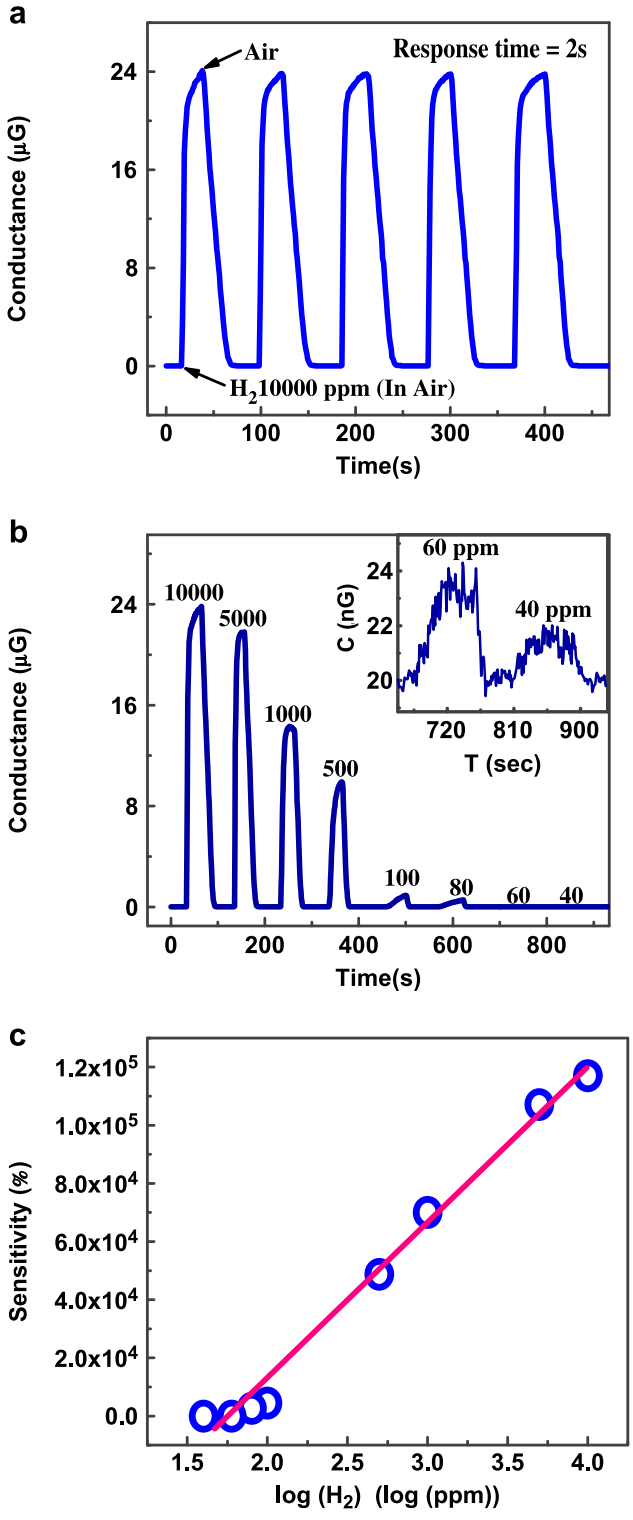

Fig. 2 – (a) A representative electrical conductance response of a SnO_2 network sensor to the presence of 10,000 ppm H_2 in air at room temperature, (b) a real-time conductance response of the SnO_2 network sensor to H_2 in the concentration range of 40–10,000 ppm in air, (c) variations of H_2 sensitivity as a logarithmic function of H_2 concentration. The inset of (b) shows the electrical conductances and the sensitivities of the SnO_2 network sensors with a H_2 concentration range of 40–60 ppm.

a function of H_2 concentration is shown in Fig. 2 c. The sensitivity (S) of the network sensor is defined as

$$S = \frac{(G_{H_2} - G_{\text{Air or } N_2})}{G_{\text{Air or } N_2}} \times 100\ (\%) \quad (1)$$

where G_{H_2} and G_{Air} are the conductance in the presence of H_2 and air, respectively. According to the definition of sensitivity, the SnO_2 network sensor was found to have $S = 1.2 \times 10^5\%$ at 10,000 ppm H_2 and $S = 10\%$ at 40 ppm H_2 in air at room temperature. Also, the sensitivity was proportional to the logarithm of the H_2 concentration at room temperature, according to:

$$S \sim A\log H_2 + B \quad (2)$$

where H_2 is the hydrogen concentration (ppm), and A and B are temperature-dependent constants. The correlation between the sensitivity and H_2 concentration was found to be in good agreement with Equation (2) in the range of 40–10,000 ppm, indicating that the SnO_2 network could be used as an H_2 sensor to effectively detect H_2 over a wide concentration range at room temperature. The representative electrical responses and the sensitivities in the presence of 10,000 ppm H_2 at room temperature for the SnO_2 network sensor in air and in N_2 are presented in Fig. 3. The H_2 sensing properties in N_2 (without O_2) were found to be much higher sensitivity than those in air. However, the conductance of the SnO_2 network sensor in N_2 was found to be partially recoverable with and without H_2.

3.2. *H_2 sensing mechanism*

We believe that O_2 plays an important role in recovering the SnO_2 network sensor after exposure to H_2 gas. Oxygen atoms are reduced to O^- ions by electrons generated from hydrogen atoms on Pd surface. The chemical reactions involved during the hydrogen gas sensing are summarized by following reactions from eqs. (3–5).

$$H_2 \rightarrow 2H \quad (3)$$

$$2H \rightarrow 2H^+ + 2e^- \quad (4)$$

$$O_2 + 2e^- \rightarrow 2O^- \quad (5)$$

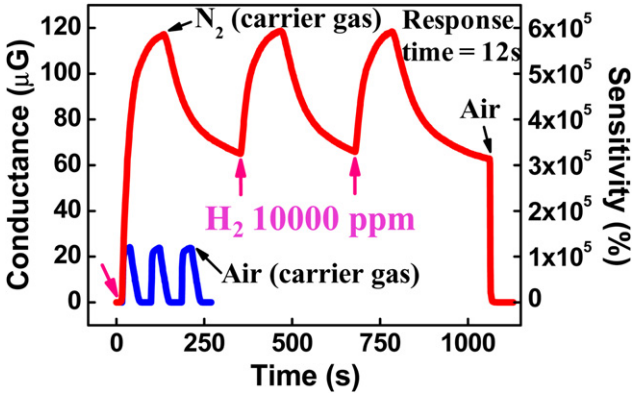

Fig. 3 – Variations in conductance and H_2 sensitivity as a function of time upon exposure to 10,000 ppm H_2 in air and in N_2, respectively.

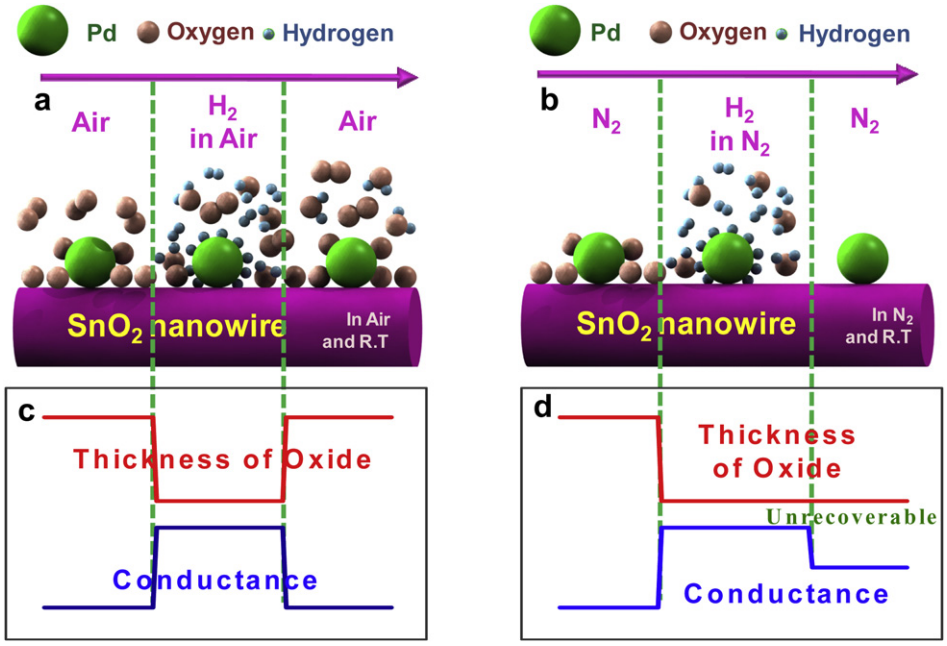

Fig. 4 – The schematic images of the SnO_2 network sensors completing one hydrogen cycle (a) in air and (b) in N_2, respectively. And the changes in conductance and of the oxide thickness (c) in air and (d) in N_2, respectively.

Eqs. (3) and (4) describe that H_2 molecules dissociate into hydrogen atoms on the surfaces of Pd NPs at room temperature and donate electrons to SnO_2 NWs. Eq. (3) is reflected by spilled-over hydrogen atoms on the surface of Pd NPs. The increased conductivity indicate that increase carrier density of n-type semiconducting SnO_2 NWs by spilled-over hydrogen atoms on the surface of Pd NPs as reflected in Eq. (4). When the SnO_2 network sensors are exposed to air, the change in conductance turns back to the initial state (OFF switching mode). Eq. (5) describes the formation of oxide from oxygen molecules from air electronically recovering wires. These reactions from eq. (5) interrupt the increase in conductance of the sensor with H_2. Therefore, the sensitivity in air is about six times lower than that in nitrogen exposure due to O_2 molecules (see Fig. 3).

The schematic images of the spill-over mechanism are presented in Fig. 4 a and b. Hydrogen and O_2 molecules dissociate into atoms on the surfaces of Pd NPs and SnO_2 wires. Fig. 4 c and d illustrate the conductance changes and the oxide thicknesses in the presence of H_2 gas in air and in N_2, respectively. After completing one cycle in N_2, the conductance and the oxide thickness did not recover to their initial values (see Fig. 4 d) and only partially recoverable, as seen in Fig. 3. Schottky barrier formation can be influenced by the work function of Pd NPs under H_2 exposure. Hydrogen molecules that dissociate into atomic hydrogen on and dissolve into Pd NPs lower the work function of the Pd [22], which may cause changes in the electron-depleted regions on n-type SnO_2. Therefore, the SnO_2 network sensor could be affected by the H_2-induced changes in the depletion regions around the Pd NPs. These phenomena can also explain the partial recovery in the absence of oxygen, as seen in Fig. 3. The proposed mechanisms can explain the on–off response, the highly changing conductance and the very fast response time of the SnO_2 network sensors in air and N_2 ambient conditions.

For recovery of sensor, electrons should be removed from the n-type SnO_2 wires. Since the SnO_2 wires were heated under the Ar gas, oxygen defect sites on the surface SnO_2 wires are abundant, which is known to activate electronic donor state increasing electronic conductivity. In recovery process, oxygen molecules from the air seem to be effectively absorbed on reduced SnO_2 wires' surface especially on the oxygen defect sites making activated oxygen species and draw electrons, which results in the high resistance of sensor. Furthermore, our SnO_2 wires have Sn nanoparticles as well as Pd particles on the surface, which seems to make the surface of SnO_2 wires more reductive, thus more effective for spill-over of oxygen molecules.

4. Conclusions

We have investigated hydrogen gas (H_2) sensors based on Pd NP-decorated tin dioxide NWs. A simple thermal evaporation of the SnO powder yields SnO_2 wires mixed with Sn nanoparticles. SnO_2 NWs with Sn NPs were effectively decorated by the Pd NPs through a reduction process in a metal ion solution. A switch-like pattern due to H_2 exposure was observed because of the reduction/oxidation of the SnO_2 network sensors due to the "spill-over effects" and the "depletion effects". As a result, the SnO_2 network sensors were found to show ultra-high sensitivity ($\sim 1.2 \times 10^5$%) and a fast response time ($\sim$2 s) upon exposure to 10,000 ppm H_2 at room temperature. Also, the SnO_2 network sensors were found to have significant electrical conductance modulations upon exposure to extremely low concentrations (down to 40 ppm) of H_2 in air. This novel fabrication method allows the production of highly-sensitive H_2 sensors that exhibit a broad dynamic detection range, a fast response time, and an ultra-low detection limit.

Acknowledgments

This work was supported by Priority Research Centers Program (2010-0028296) through the National Research Foundation of Korea (NRF), the Basic Research Program grant (2010-0027687) and Seoul Research and Business Development Program (10816) S Kim is grateful for the financial support of a grant from the National Research Foundation of Korea Grant funded by the Korean Government (2010-0001484).

Appendix. Supplementary material

Supplementary material associated with this article can be found in the online version, at doi:10.1016/j.ijhydene.2010.08.026.

REFERENCES

[1] Goltsov VA, Veziroglu TN, Goltsova LF. Hydrogen civilization of the future—A new conception of the IAHE. Int J Hydrogen Energy 2006;31:153–9.
[2] Shukla S, Seal S, Ludwig L, Parish C. Nanocrystalline indium oxide-doped tin oxide thin film as low temperature hydrogen sensor. Sens Actuators B 2004;97:256–65.
[3] Firth JG, Jones A, Jones TA. The principles of the detection of flammable atmospheres by catalytic devices. Combust Flame 1973;21:303–11.
[4] Lewis FA. The palladium hydrogen system. London: Academic; 1967.
[5] Favier F, Walter EC, Zach MP, Benter T, Penner RM. Hydrogen sensors and switches from Electrodeposited palladium Mesowire Arrays. Science 2001;293:2227–31.
[6] Atashbar MZ, Banerji D, Singamaneni S. Room-temperature hydrogen sensor based on palladium nanowires. IEEE Sens J 2005;5:792–7.
[7] Xu T, Zach MP, Xiao ZL, Rosenmann D, Welp U, Kwok WK, et al. Self-assembled monolayer-enhanced hydrogen sensing with ultrathin palladium films. Appl Phys Lett 2005;86:203104.
[8] Dankert O, Pundt A. Hydrogen-induced percolation in discontinuous films. Appl Phys Lett 2002;81:1618.
[9] Choi YH, Yang M, Hong SH. H_2 sensing characteristics of highly textured Pd-doped SnO_2 thin films. Sens Actuators B 2008;134:117–21.
[10] De G, Kohn R, Xomeritakis G, Brinker J. Nanocrystalline mesoporous palladium activated tin oxide thin films as room-temperature hydrogen gas sensors. Chem Comm; 2007:1840–2.
[11] Shukla S, Zhang P, Cho HJ, Seal S, Ludwig L. Room temperature hydrogen response kinetics of nano micro-integrated doped tin oxide sensor. Sens Actuators B 2007;120:573–83.
[12] Martinelli G, Carotta MC. Thick-film gas sensors. Sens Actuators B 1995;23:157–61.
[13] Kolmakov A, Klenov DO, Lilach Y, Stemmer S, Moskovits M. Enhanced gas sensing by individual SnO_2 nanowires and nanobelts functionalized with Pd catalyst particles. Nano Lett 2005;5:667–73.
[14] Kolmakov A, Moskovits M. Chemical sensing and Catalysis by one-Dimensional metal-oxide nanostructures. Annu Rev Mater Res 2004;34:151–80.
[15] Shen Y, Yamazaki T, Liu Z, Meng D, Kikuta T, Nakatani N, et al. Microstructure and H_2 gas sensing properties of undoped and Pd-doped SnO_2 nanowires. Sens Actuators B 2009;135:524–9.
[16] Tan ETH, Ho GW, Wong ASW, Kawi SW. Gas sensing properties of tin oxide nanostructures synthesized via a solid-state reaction method. Nanotechnology 2008;19:255706–12.
[17] Chaudhary VA, Mulla IS, Vijayamohanan K. Comparative studies of doped and surface modified tin oxide towards hydrogen sensing: Synergistic effects of Pd and Ru. Sens Actuators B 1998;50:45–51.
[18] Suzuki T, Yamazaki T, Hayashi K, Noma T. High gas sensitivity of tin oxide ultrathin films deposited on glasses and alumina substrates. J Mat Sci 1991;26:6419–22.
[19] Jeon KJ, Jeun MH, Lee E, Lee JM, Lee KI, Allmen PV, et al. Finite size effect on hydrogen gas sensing performance in single Pd nanowires. Nanotechnology 2008;19:495501–6.
[20] Jeon KJ, Lee JM, Lee E, Lee W. Individual Pd nanowire hydrogen sensors fabricated by electron-beam lithography. Nanotechnology 2009;20:135502–6.
[21] Sears WM, Colbow K, Consadori F. Algorithms to improve the selectivity of thermally-cycled tin oxide gas sensors. Sens Actuators 1989;19:333–49.
[22] Kong J, Chapline G, Dai H. Functionalized carbon nanotubes for molecular hydrogen sensors. Adv Mater 2001;13:1384–6.